

MITIGATION OF THE SEISMIC MOTION APPLIED NEAR A SLOPE USING ANCHORS AND PILES

Constantine STAMATOPOULOS¹, Maria BASSANO¹

ABSTRACT

Buildings near the edge of slopes suffer serious damage, presumably as a result of amplification of the acceleration near the edge of the slope. The paper studies the effect of mitigating this amplification of acceleration by adding anchors or piles at the vicinity of a building at the crest and near the edge of the slope. If we connect the part in which topographic amplification occurs to that in which it doesn't then clearly the accelerations have to become more uniform. Dynamic elasto-plastic numerical analyses were performed. They illustrated that without mitigation, the topography amplifies considerably the acceleration at the location of the building under two input earthquake motions. Parametric analyses illustrated the optimum configuration for the mitigation measures considered. When the optimum mitigation configurations are applied, the intensity of the seismic motion below the building approaches the levels of the 1-dimensional case far away from the edge of the slope, by about 50% or more.

Keywords: topographic amplification, mitigation, piles, anchors, finite element dynamic analyses

1. INTRODUCTION

Concentration of damage of buildings near the edge of hard or dense natural slopes has been observed during a number of recent earthquakes (Athanasopoulos et al, 1999, Assimaki et al, 2005). This observation has been interpreted by numerical dynamic analyses that illustrate the amplification of the horizontal acceleration near the edge of slopes (Athanasopoulos et al, 1999, Assimaki et al, 2005, Bouckovalas and Papadimitriou, 2005). Methods mitigating the topographic effect described above do not exist in the literature. Such methods are needed in cliffs with existing buildings that are not designed to sustain the very large anticipated total and differential accelerations in the case of a near seismic event.

The purpose of this paper is to study the effect of two mitigation measures to decrease the severity of the seismic motion at a particular location. The location considered is a simplified simulation of the eastern part of the slope at Aegion city, Greece. At this region, a four-floor reinforced concrete building located 10 to 25m from the edge of the slope, under construction at the time of the 1995 Aegion earthquake, was severely damaged and required major repairing. More details of this case study are given by Stamatopoulos et al (2005). The seismic acceleration just below this building is considered.

Two mitigation measures are studied numerically: (a) anchors and (b) piles. The intensity of the seismic motion may be reduced by anchors or piles placed on the crest and near the edge of the slope because the region at the crest near the edge where accelerations are higher is connected to the region at some depth where accelerations are lower. In this manner, the whole body connected with anchors will move in a uniform manner with reduced maximum and differential accelerations. Anchors of

¹ Stamatopoulos and Associates Co, 5 Isavron street, Athens 11471, Greece, Email : kstamato@tee.gr

similar length have lower cost than piles, by a factor of about 50%. On the other hand, as piles can have larger cross-sectional diameter than anchors, it is anticipated that they may prove more efficient.

2. CHARACTERISTICS OF THE SITE AND EARTHQUAKES CONSIDERED

Topographic mapping of the eastern part of the Aegion slope was performed by the Institute of Geology and Mineral Exploration of Greece (IGME). A geotechnical investigation including borings near the edge and at the base of the slope was also performed by IGME. The water table was found at depth about 40m below the crest and 5m below the base of the slope. The geotechnical profile below the crest consists of soil that extends to a depth of 32m. Based on the above, figure 1 gives a simplified 2-dimensional cross-section and profile of shear velocity, V_s , of the area.

It is a low-plasticity clay layer, except for a surface fill layer 3m deep. Below the base of the slope, the clay layer extends to a depth of 20m. Geophysical tests have been performed in the region by previous investigators. They are reported by Athanasopoulos et al (1999) and Bouckovalas et al (1999).

In the laboratory of Stamatopoulos and Associates Ltd tests were performed on soil samples retrieved from the borings. Classification tests revealed a mean Plasticity Index (PI) value of 7 for the top fill layer and a mean PI value of 10 for the clay layer below. Drained triaxial tests gave for the top fill layer peak strength parameters of $\phi=34^\circ$, $c=45\text{kPa}$ and for the low-plasticity clay layer below $\phi=35^\circ$, $c=30\text{kPa}$.

Similarly to previous analyses of the Aegion slope during the 1995 earthquake (Athanasopoulos et al, 1999) (a) only horizontal motion is considered and (b) the input motion for the calculations is based on the record obtained at the basement of the building of OTE (given e.g. by Bouckovalas et al, 1999). The base motion is such that when propagated through the 2-D model generates a response at the OTE site similar to the one recorded during the 1995 earthquake. As the OTE site is located a large distance (about 200m) from the edge of the slope and the recording was at the basement of the OTE building, it is assumed that wave propagation is 1-dimensional and soil-structure interaction effects can be neglected. Therefore, the base motion was obtained by 1-dimensional equivalent-linear deconvolution. The code Cyberquake (BRGM software, 1998) was used for this purpose. The deconvoluted input is shown in figure 2a.

Numerical analyses using another base motion were also performed to check the influence of the input motion in the results. The Friuli-San Rocco-Italy 15/9/76 earthquake (y-y horizontal component), shown in figure 2b, was applied in the horizontal direction. The Friuli earthquake was selected because its dominant period is 0.20s, typical for Europe, and considerably less than the dominant period of the Aegion earthquake (0.42s).

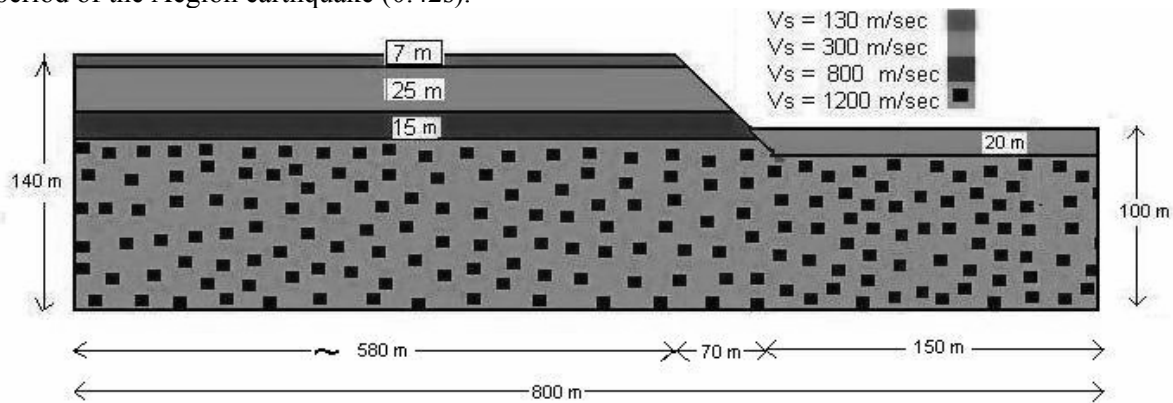


Figure 1. Site topography and V_s profile used in the analyses

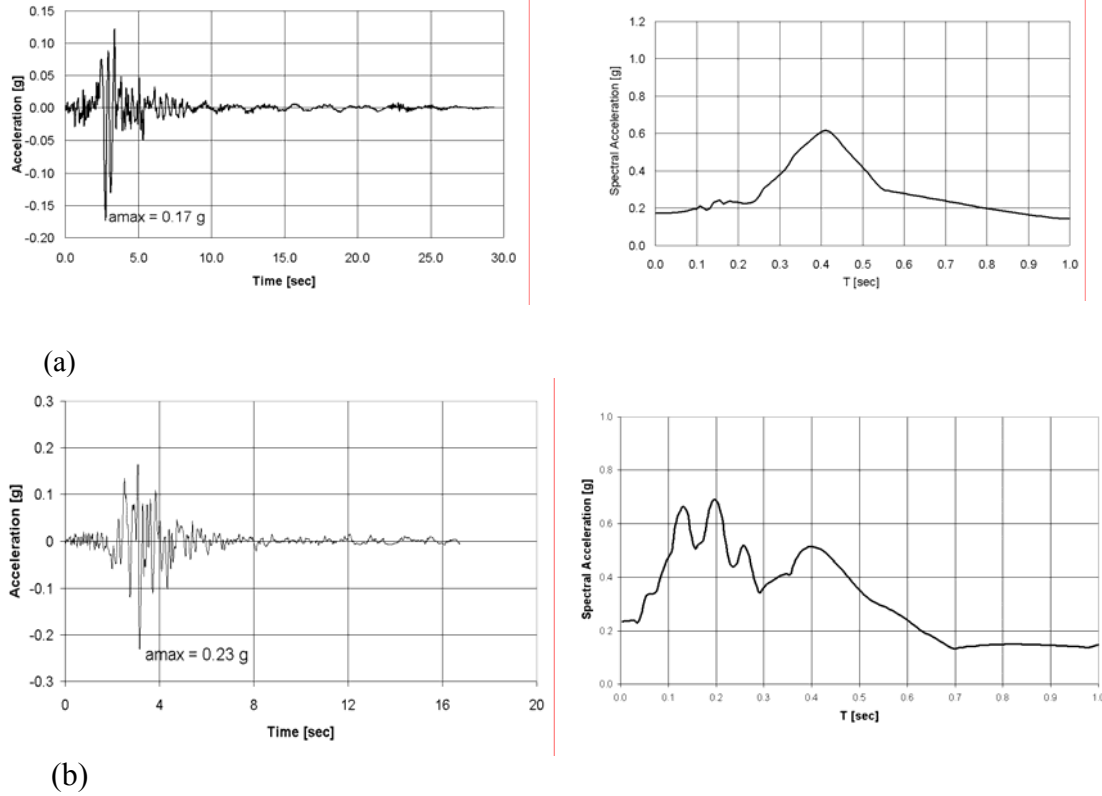


Figure 2: Input accelerations applied at this study: (a) the decomvoluted Aegion 1995 earthquake and (b) Friuli 1976 earthquake. Both the acceleration histories and the response spectra at 5% damping are given

3. NUMERICAL ANALYSES

3.1 Numerical analysis procedure

The elasto-plastic model that was used in the analysis is similar to that presented and validated by Stamatopoulos et al (2005b). The method is a simplified version of the model developed at Ecole Centrale Paris and described by Aubry et al (1993). It has been calibrated in terms of soil type by Modaressi and Lopez-Caballero (2001). Soil response under drained conditions is predicted by the following equations:

$$(1) \quad \tau / \sigma' = F \tan \phi_{cs} \left[\gamma^p / (\tan \phi_{cs} / E_p + \gamma^p) \right]^{0.5} \quad \text{where}$$

$$F = 1 - b \ln (\sigma' / \sigma'_c)$$

$$\sigma'_c = \sigma_{co} \exp (-\beta \varepsilon_v^p)$$

$$\varepsilon_v^p = \gamma^p (\tan \phi_{cs} + \tau / \sigma') \quad \text{for } \gamma^p > \gamma_{mob}$$

In the above equations τ and σ' are the shear and effective normal stress at the failure plane, ϕ_{cs} , β , E_p , γ_{mob} , b and σ_{co} are model parameters and ε_v^p and γ^p are the volumetric and shear plastic strain. The model is based on (a) the critical state theory that predicts that soil response is affected by the distance from the critical state (The factor F gives the distance from the critical state), (b) the fact that plastic shear strain depends on the τ / σ' ratio and (c) a Roscoe type dilation equation. Modaressi and Lopez-Caballero (2001), give typical values of the parameters ϕ_{cs} , β , E_p , γ_{mob} , b for sands and clays. The parameter σ_{co} depends on sand density or clay precompression value.

The above expressions under cyclic loading do not simulate kinematic hardening: the response during unloading and reloading when the past peak stress ratio is not exceeded is assumed elastic. For this reason, when dynamic analysis is performed, damping should not have its elastic value, but a larger value corresponding to the magnitude of shear stress applied at these cycles. In particular, for the 1-dimensional case of level ground, comparison of predictions of the proposed method with the shear velocity (V_s) profile of figure 1 with those of the equivalent-linear dynamic method performed by the computer code Cyberquake (BRGM software, 1998) has illustrated that the Rayleigh damping value of 0.07 gives similar results.

Soil extends over only the two top layers of figure 1, the underlying formations being soft rock. Table 1 gives the values of the parameters of the elasto-plastic model of equations (1) and (2) that were selected for these soft layers for the numerical analyses. The values of the parameters ϕ_{cs} , β , E_p , γ_{mob} , b are similar to those proposed by Modaressi and Lopez-Caballero (2001) in terms of the plasticity index of the soil. The value of σ_{co} was selected in order to predict the peak soil strength that was measured in the drained tests, in terms of the applied stress. As illustrated in figure 3, these expressions and parameters predict (a) the measured peak shear strength, (b) the measured soil softening (i.e. degradation of soil strength with further straining), (c) the measured dilation and (d) the decrease of the "equivalent" shear modulus with the applied shear strain as predicted e.g. by the relationships of Ishibashi and Zhang (1993), in terms of the plasticity index of the soil.

The numerical code FLAC (Itasca Consultants, 2002) was used in the analyses. The elasto-plastic model described by equations (1) and (2) was applied at the soil layers using the SS (Strain Hardening-Softening) elasto-plastic model that is included in the FLAC code. Application was made using the equivalent relationship of (a) the friction ($=\text{atan}(\tau/\sigma')$) and (b) the dilation angles in terms of the plastic shear strain. As small strains are anticipated in the soft rock layers below the two soil layers, these layers were simulated using elastic models.

The building near the edge of the slope was also simulated. It was modeled as the simple structure consisting of beam elements shown in figure 4. Beam elements are included in the FLAC code. The parameters that were used are typical for beams: density= 1900Kg/m^3 , Young modulus= $35*10^9\text{Pa}$, cross sectional area= $4.8*10^{-3}\text{m}^2$, inertia = $2.3*10^{-5}\text{m}^4$. Vertical loads of $-2*10^4\text{N}$ per floor were applied simulating the dead and live loads of each floor, per meter in the direction not shown in figure 4.

To simulate the mitigation measures, anchors and piles are applied using the structural cable and pile elements that are included in the FLAC code. Cable elements that correspond to anchors are 1d axial elements that may be anchored at a specific grid point or grouted. These elements that can yield in tension or compression and are used to model a variety of supports where tensile capacity is important, including anchors. Pile elements are 2d elements that can transfer normal and shear forces and bending moments to the grid. As far as the cable properties is concerned, in addition to the length and cross-sectional area, the following properties are needed: (a) density, (b) Young modulus, (c) tensile yield strength, (d) friction angle at the interface, (e) cohesive strength of the grout and (f) stiffness of the grout. For the piles, in addition to the length and cross-sectional area, the following pile properties are needed: (a) density, (b) Young modulus (c) stiffness of the shear coupling spring, (d) frictional and cohesional resistance of the shear coupling spring, (e) stiffness of the normal coupling spring, (f) frictional and cohesional resistance of the normal coupling spring. Yet, the frictional and cohesional resistance of the shear coupling spring correspond to those of the soil and the properties (e) and (f) can be obtained from the other pile properties (Itasca Consultants, 2002).

Two-dimensional plane strain analyses were performed. The spacing of beams, piles and anchors in the direction not given in figure 4 is simulated by FLAC using appropriate scaling rules for the anchor sizes and properties (Itasca Consultants, 2002).

Table 1: The values of the parameters of the elasto-plastic model used in the numerical studies.

| Layer | Fill (depth 0 to 2m below the top of the slope) | Clay |
|-----------------|---|-----------|
| $\phi [^\circ]$ | 30 | 30 |
| β | 23 | 23 |
| σ_∞ | 250 kPa | 400 kPa |
| E_p | 220 kPa | 220 kPa |
| γ_{mob} | 10^{-3} | 10^{-3} |
| b | 1.0 | 1.0 |

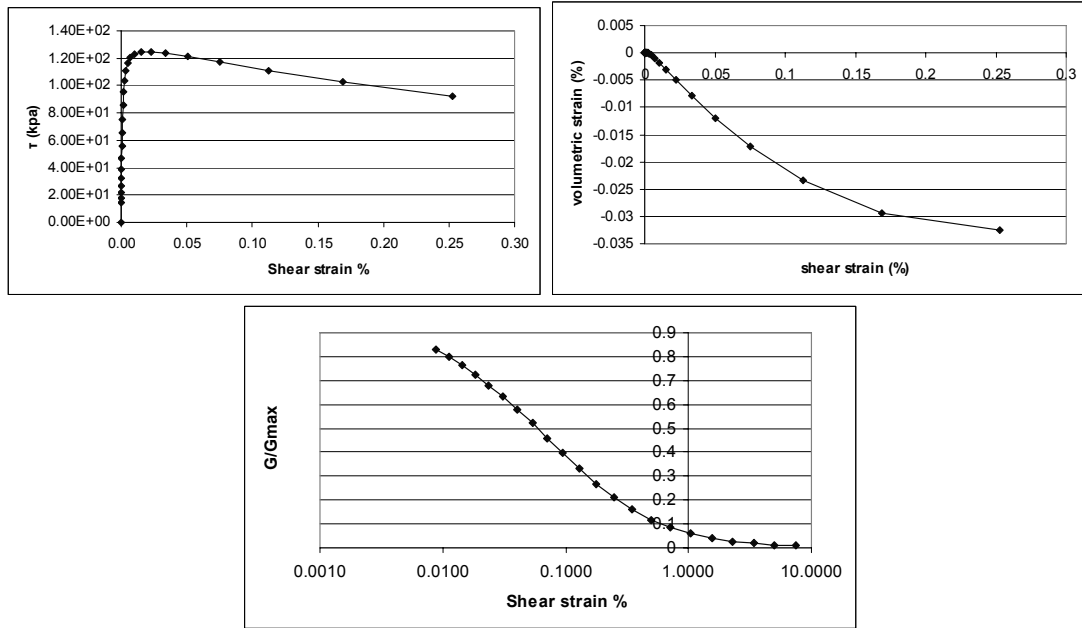


Figure 3. Predictions of the model with the proposed model parameters. The case of the clay layer at $\sigma' = 140 \text{ kPa}$ is presented.

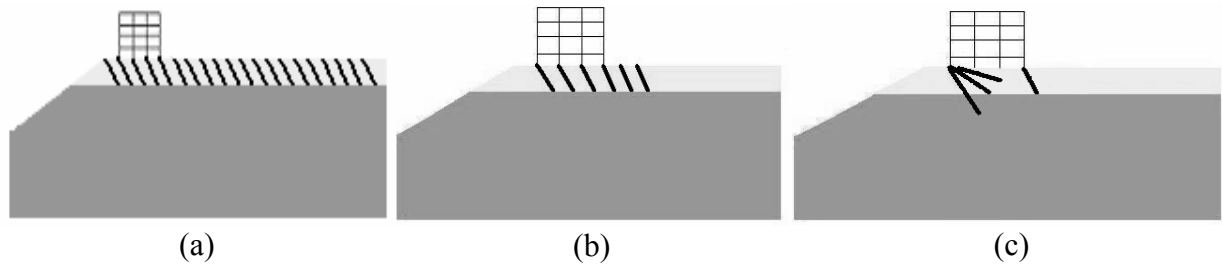


Figure 4: The building and mitigation configurations considered in the present analysis (a) using uniformly-spaced anchors, (b) using uniformly-spaced piles, (c) using piles only at the corners of the building

3.2 No mitigation case

The profile shown in figure 1 was applied. It extends horizontally 600m from the edge, in order to capture the 1-dimensional response far away from the edge. A number of different meshes were designed and used in order to validate the results. In the presented analysis, the mesh had about 2000 elements and was finer near the edge of the slope. The vertical size of the finite elements was less than 2m, appropriately smaller than one tenth of the minimum critical wavelengths that are expected to be developed during the seismic excitations. Viscous dampers are used at the lateral boundaries of the mesh. This avoids undesirable reflections of the outgoing waves.

Five different layers were assumed: the upper fill layer, two sub-layers simulating the clay layer with different shear moduli, and two layers simulating the soft rock below, also with different shear moduli. The elastic moduli were taken according to the V_s values of figure 1. The elasto-plastic parameters for the soil layers were taken as given in table 1. Based on the above discussion, Rayleigh damping with damping coefficient of 0.07 was used. Finally, similarly to practice in numerical analysis, a Poisson ratio equal to 0.3 was used.

The numerical analysis was performed in two steps: First gravity was applied and the static stresses were computed. Then the earthquakes of figures 2a or 2b were applied at the base of the grid. Figures 5a and 5b give the computed acceleration histories for the Aegion earthquake at zero depth (a) 10m from the edge of the slope and (b) 200m from the edge of the slope. Figure 5c presents the computed settlement versus time at the crest of the slope and at distance 10m from the edge for the Aegion earthquake.

Figures 6a and 6b give the computed horizontal acceleration spectra of the seismic motion for the Aegion and Friuli earthquakes respectively at the surface of the slope. Figures 7 and 9 give the computed maximum horizontal acceleration and final settlement at the surface of the slope in terms of horizontal distance from the edge of the slope for both earthquakes. Figures 8a and 8b give the peak horizontal acceleration versus the horizontal distance from the edge of the slope below the building at distances 0 to -40m for both earthquakes. These figures are a detail of figures 7a and 7b. Table 2 gives the computed maximum horizontal acceleration and maximum horizontal spectral acceleration below the building for both earthquakes.

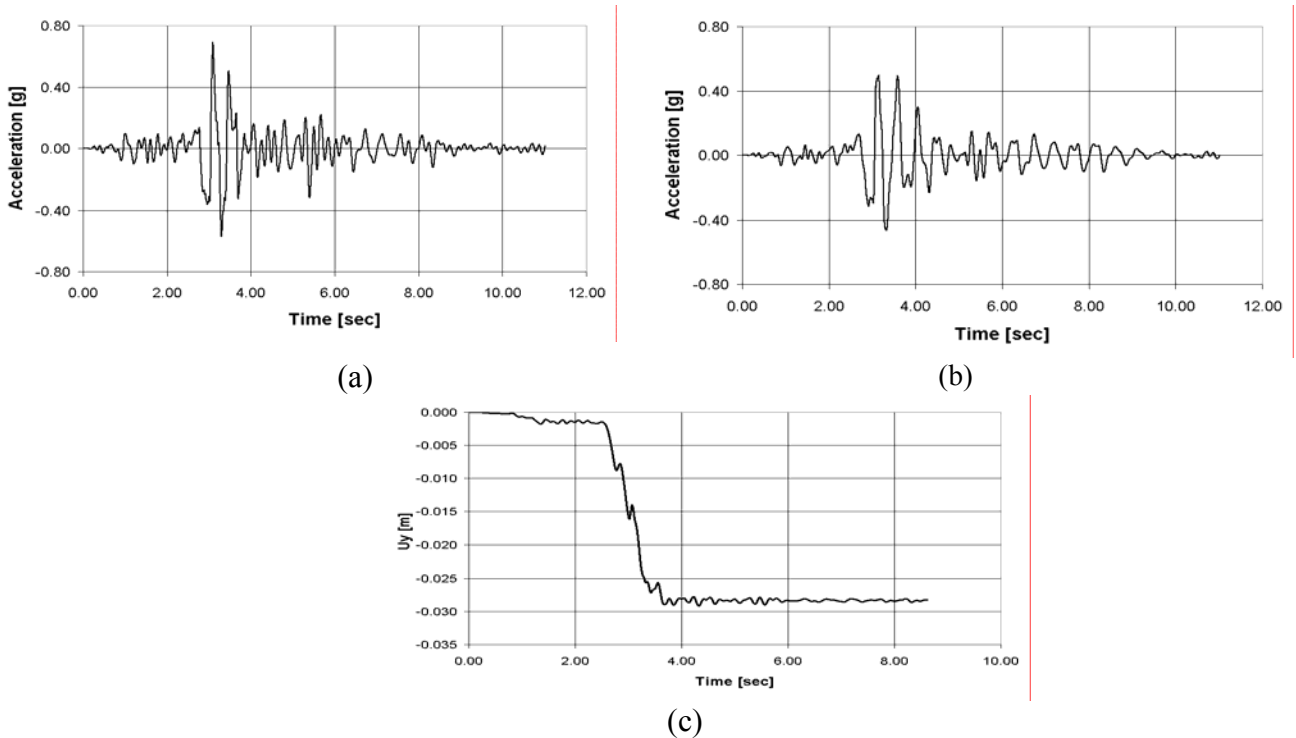
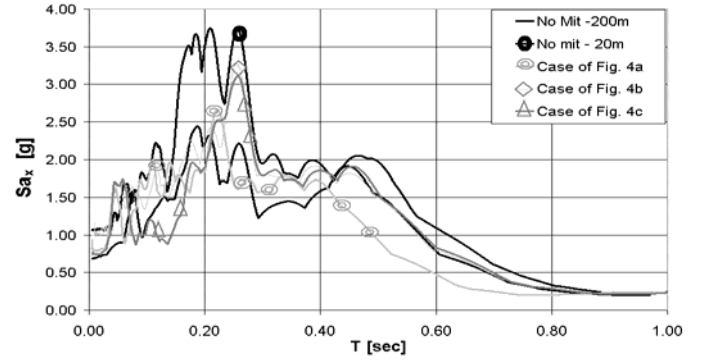
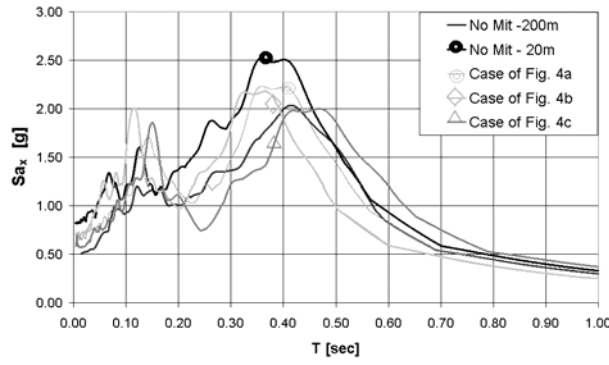
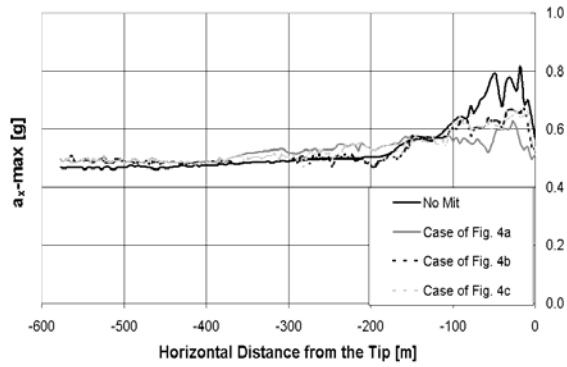


Figure 5. The case without mitigation and the Aegion earthquake. Acceleration history (a) 10m from the edge of the slope and (b) 200m from the edge of the slope. (c) Computed settlement with time (negative U_y means positive settlement), 10m from the edge.



(b)

Figure 6. Acceleration spectra for the cases without and with mitigation. (a) Aegion and (b) Friuli earthquakes. "No Mit" indicates the case without mitigation.



(a)

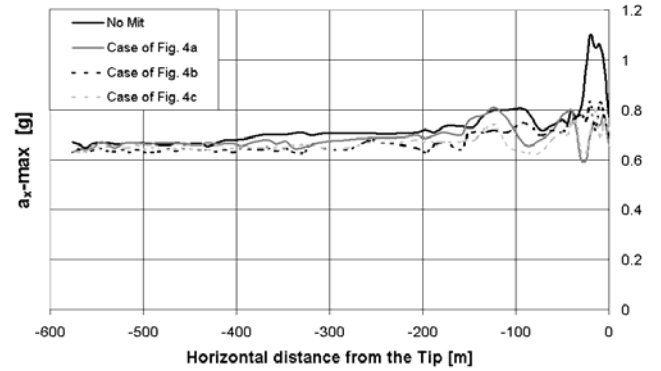
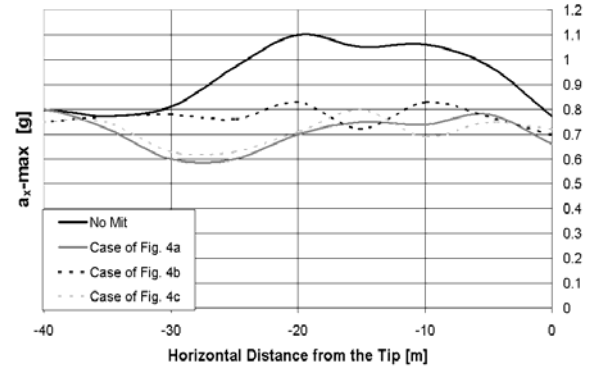
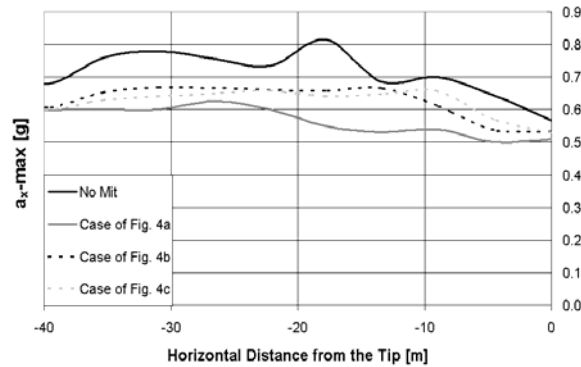
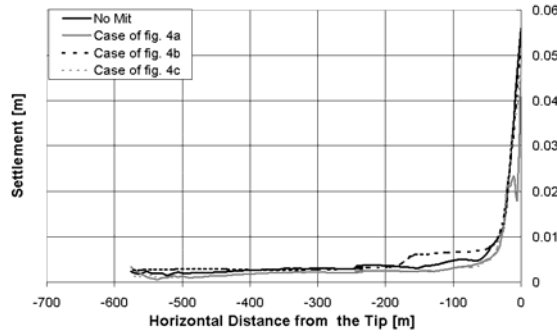


Figure 7. Peak horizontal acceleration versus the horizontal distance for the cases without and with mitigation for (a) the Aegion and (b) the Friuli earthquakes.

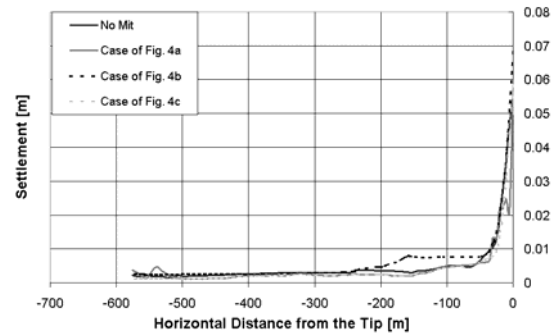


(b)

Figure 8. Peak horizontal acceleration versus the horizontal distance from the edge of the slope below the building at distances 0 to -40m for (a) the Aegion and (b) the Friuli earthquakes. This figure is a detail of figure 7.



(a)



(b)

Figure 9. Final settlement versus the horizontal distance from the edge of the slope for the cases both without and with mitigation at zero depth for (a) the Aegion and (b) the Friuli earthquakes.

Table 2. The topographic effect and effect of mitigation measures in the cases considered. The TE and ME factors are defined by equations (2) and (3) respectively.

(a) a_{x-max} [g]

| Case | 1-D* | 2-D no mitigation ** | 2-D with mitigation | TE- a_x factor | ME- a_x factor |
|-----------------------------|------|----------------------|---------------------|------------------|------------------|
| Aegion earthquake - fig. 4a | 0.50 | 0.82 | 0.63 | 1.63 | 0.60 |
| Aegion earthquake - fig. 4b | 0.50 | 0.82 | 0.66 | 1.63 | 0.49 |
| Aegion earthquake - fig. 4c | 0.50 | 0.82 | 0.65 | 1.63 | 0.53 |
| Friuli earthquake - fig. 4a | 0.72 | 1.10 | 0.74 | 1.53 | 0.95 |
| Friuli earthquake - fig. 4b | 0.72 | 1.10 | 0.83 | 1.53 | 0.71 |
| Friuli earthquake - fig. 4c | 0.72 | 1.10 | 0.69 | 1.53 | 1.08 |

(b) Sa_{x-max} [g]

| Case | 1-D* | 2-D no mitigation ** | 2D with mitigation | TE- Sa_x factor | ME- Sa_x factor |
|-----------------------------|------|----------------------|--------------------|-------------------|-------------------|
| Aegion earthquake - fig. 4a | 2.02 | 2.5 | 2.22 | 1.24 | 0.58 |
| Aegion earthquake - fig. 4b | 2.02 | 2.5 | 2.17 | 1.24 | 0.69 |
| Aegion earthquake - fig. 4c | 2.02 | 2.5 | 2.00 | 1.24 | 1.04 |
| Friuli earthquake - fig. 4a | 2.40 | 3.7 | 2.64 | 1.54 | 0.82 |
| Friuli earthquake - fig. 4b | 2.40 | 3.7 | 3.10 | 1.54 | 0.46 |
| Friuli earthquake - fig. 4c | 2.40 | 3.7 | 3.07 | 1.54 | 0.48 |

* 200m from the edge for the case without mitigation

** maximum response 10 to 25m from the edge

3.3 Mitigation with anchors

The profile considered and the anchors were modelled as described in sections 3.1 and 3.2. A large number of parametric analyses were performed. These parametric analyses illustrated that: (a) the response does not change considerably when the diameter and material properties of the anchors vary within the range of possible values (diameter between 0.05 and 0.4m, bond friction between 0 and 45°, tensile yield strength between 10^8 and 10^{10} N, stiffness of the grout between 0 and 10^{10} Pa, cohesive strength of the grout between 0 and 10^4 Pa, Young modulus between 10^7 and 10^{12} Pa) and (b) the response depends on the inclination, the length and the spacing of the anchors. Optimum inclination angle of anchors is 55° to the horizontal and optimum anchor length is about 6m. For best cost-effective

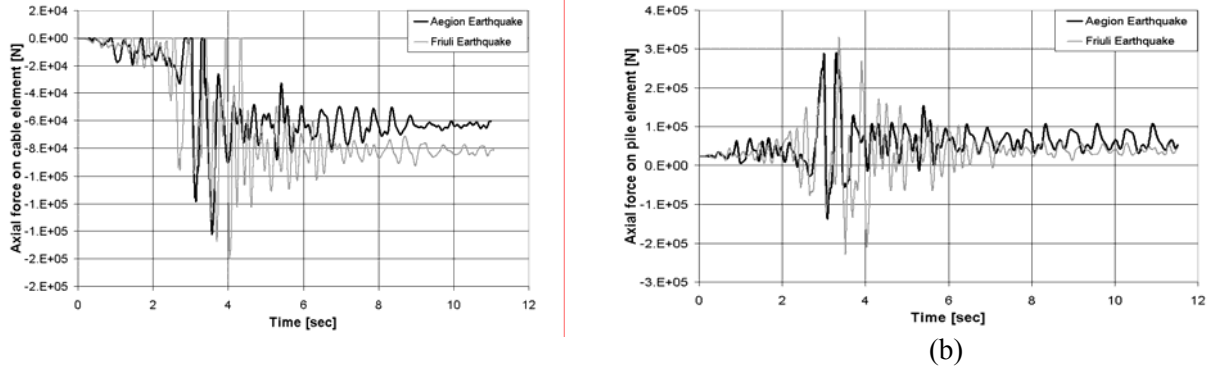


Figure 10. (a) Axial forces on the mid-point of the anchor below the right edge of the building for case (a) of figure 4. (b) Axial forces on the mid-point of the pile below the right edge of the building for case (b) of figure 4. Results for both the Aegion and the Friuli earthquakes are given.

results, for uniform anchor spacing, anchors must be parallel to each other. As number of anchors increases, the seismic accelerations near the edge decrease more.

The optimum configuration obtained for uniform anchor spacing of 5m mitigating considerably the seismic motion below the building is given in figure 4a. There are 20 anchors with 55° inclination to the horizontal. For this configuration, figures 6a and 6b give the computed horizontal acceleration spectra of the seismic motion for the Aegion and Friuli earthquakes respectively at the surface of the slope. Figures 7 and 9 give the computed maximum horizontal acceleration and final settlement at the surface of the slope in terms of horizontal distance from the edge of the slope for both earthquakes. Figures 8a and 8b give the peak horizontal acceleration versus the horizontal distance from the edge of the slope below the building at distances 0 to -40m for both earthquakes. These figures are a detail of figures 7a and 7b. Figure 10 gives the computed axial force versus time in the mid-point of the anchor below the right edge of the building for case (a) of figure 4 for the Aegion and the Friuli earthquakes. Table 2 gives the computed maximum horizontal acceleration and maximum horizontal spectral acceleration below the building for both earthquakes. Anchor characteristics assumed were: density= 7000Kg/m^3 , Young modulus= $2.1 \times 10^{11}\text{Pa}$, diameter = 0.05m, tensile yield strength= $2.3 \times 10^6\text{N}$, stiffness of the grout= $7 \times 10^6\text{Pa}$, cohesive strength of the grout= 10^2Pa . These anchor properties are typical of those in current practice. Anchors are assumed every five meters in the direction not shown in figure 4.

3.4 Mitigation with piles

The profile considered and the piles were modelled as described in sections 3.1 and 3.2. More than fifty arithmetic analyses were performed by varying pile properties, number of piles, pile locations, pile length, piles diameter, pile inclination. Many properties of piles are more-or-less fixed and cannot be changed considerably. These include density, Young modulus, stiffness of the equivalent shear springs, friction, cohesion. Parametric analyses were performed to investigate whether the response changes if these parameters vary by a small amount, and it was found that they do not change considerably. The parametric analyses illustrated that the response depends on the inclination, the length and the spacing of the piles. Optimum inclination angle of piles is about 55° to the horizontal and optimum pile length is about 6m. As number of piles increases, the seismic accelerations near the edge decrease more.

The optimum configuration obtained with uniform pile spacing of 5m mitigating considerably the seismic motion below the building is given in figure 4b. There are 6 piles of 5 m length, 0.8 m diameter and 55° inclination. Yet, this configuration has the disadvantage that it requires installation of piles below the building. An alternative possible arrangement of piles of similar diameter that can be constructed entirely on the outside of the building, is shown in figure 4c.

For the pile configurations of figures 4b and 4c, figures 6a and 6b give the computed horizontal acceleration spectra of the seismic motion for the Aegion and Friuli earthquakes, respectively, at the surface of the slope. Figures 7 and 9 give the computed maximum horizontal acceleration and final settlement at the surface of the slope in terms of horizontal distance from the edge of the slope for both earthquakes. Figures 8a and 8b give the peak horizontal acceleration versus the horizontal distance from the edge of the slope below the building at distances 0 to -40m for both earthquakes. These figures are a detail of figures 7a and 7b. Figure 10 gives the computed axial force versus time in the mid-point of the pile below the right edge of the building for case (b) of figure 4 for the Aegion and the Friuli earthquakes. Table 2 gives the maximum horizontal acceleration and maximum horizontal spectral acceleration below the building for both earthquakes. Pile characteristics assumed were: density=3000Kg/m³, Young modulus=200*10⁹Pa, stiffness of the shear springs=4*10⁶Pa, friction=30°, cohesion=0. These pile properties are typical of those in current practice. Piles are assumed every five meters in the direction not shown in figure 4.

4. DISCUSSION

4.1 General

The topographic effect is described in the present study by considering the amplification of both the maximum horizontal acceleration (a_{x-max}) and the maximum spectral horizontal acceleration (Sa_{x-max}). The following dimensionless factors are used:

$$(2) \quad \begin{aligned} TE-a_x &= a_{x-max-2D} / a_{x-max-1D} \\ TE-Sa_x &= Sa_{x-max-2D} / Sa_{x-max-1D} \end{aligned}$$

where the subscript 1D indicates the response far away from the edge where the topographic effect does not exist, while the subscript 2D indicates the maximum response below the building of figure 4, near the edge of the slope.

To quantify the effect of the mitigation measures, the following dimensionless factors are defined:

$$(3) \quad \begin{aligned} ME-a_x &= (a_{x-max-nomit} - a_{x-max-mit}) / (a_{x-max-nomit} - a_{x-max-1D}) \\ ME-Sa_x &= (Sa_{x-max-nomit} - Sa_{x-max-mit}) / (Sa_{x-max-nomit} - Sa_{x-max-1D}) \end{aligned}$$

where the subscripts max-nomit and max-mit indicate the maximum values attained below the building near the edge of the slope for the no mitigation case and the mitigation cases respectively.

The ME factors are equal to 0 if the mitigation method has no effect and 1 if the mitigation method completely eliminates the topographic effect. They take values greater than one when the mitigation measure reduces the response near the edge to values less than far away from the edge.

4.2 No mitigation case

The Aegion geometry numerical analyses indicated that when base maximum acceleration is 0.17g and 0.23g for the Aegion and Friuli earthquakes respectively, maximum acceleration at the surface 200m from the toe ($a_{x-max-1D}$) equals about 0.50g and 0.72 g for the Aegion and Friuli earthquakes respectively. The maximum spectral acceleration at the surface 200m from the toe ($Sa_{x-max-1D}$) equals 2.02g and 2.40g respectively.

As illustrated in table 2, below the building considered, near the edge of the slope, the factor $TE-a_x$ equals 1.63 and 1.53 for the Aegion and Friuli earthquakes respectively. Regarding the spectral response, the factor $TE-Sa_x$ equals 1.24 and 1.54 respectively. Furthermore, the permanent settlements below the building were small for both earthquakes (less than 5cm).

These values of the TE factors illustrate the importance of the topographic effect in increasing the horizontal peak acceleration and peak spectral acceleration. It should be noted that these amplification factors are in general agreement with the findings of previous analyses of the topographic effect (Assimaki et al, 2005, Bouckovalas and Papadimitriou, 2005).

4.3 Effectiveness of the mitigation methods

The numerical analyses illustrated that the seismic motion below the building can be mitigated if an adequate number of anchors or piles is used. The peak value of acceleration near the edge of the slope is reduced and a more uniform acceleration pattern is produced: As illustrated in table 2, for the mitigation measure of figure 4a, the factor $ME-a_x$ equals 0.60 and 0.53 for the Aegion and Friuli earthquakes respectively, while the factor $ME-Sa_x$ equals 0.58 and 0.82 respectively. For the mitigation measure of figure 4b the factor $ME-a_x$ equals 0.49 and 0.71 for the Aegion and Friuli earthquakes respectively, while the factor $ME-Sa_x$ equals 0.69 and 0.46 respectively. For the mitigation measure of figure 4c, the factor $ME-a_x$ equals 0.53 and 1.08 for the Aegion and Friuli earthquakes respectively, while the factor $ME-Sa_x$ equals 1.04 and 0.48 respectively. Comparing the three mitigation geometries considered, it can be observed that the mitigation measure of figure 4c is the most effective (average ME factor is 0.78), next follows the mitigation measure of figure 4a (average ME factor equals 0.74) and next is the measure of figure 4b (average ME factor equals 0.60).

Concluding, the numerical analysis of the Aegion slope illustrated that anchors or piles can mitigate considerably the amplification of the horizontal acceleration near the edge. For both earthquakes, the mitigation decreased the topographic effect in terms of horizontal accelerations by about 50% or more. More specifically, in the cross-section of the slope, 20 anchors 5m apart proved more effective than 6 piles of similar length and spacing. More dense spacing near the building was even more effective in mitigating the seismic motion below the building.

4.4 Reason for the effectiveness of the mitigation methods

The main issue is that different regions of the slope have different acceleration fields. Therefore if we connect the part in which topographic amplification occurs to that in which it doesn't then clearly the accelerations have to become more uniform. This is what is observed in the results. Alternatively it can be stated that the specific use of anchors increases the rigidity of the surface layer introducing an "equivalent" stiffer "reinforced soil" that extends to a depth of about 5m. Proof that anchors work is that axial forces of anchors/piles are generated during shaking.

5. CONCLUSIONS

Buildings near the edge of slopes suffer serious damage presumably as a result of amplification of the acceleration near the edge of the slope. The paper studies the effect of mitigating this amplification of acceleration at the vicinity of a building by adding anchors or piles at the crest and near the edge of the slope. The main issue is that different regions of the slope have different acceleration fields. Therefore if we connect the part in which topographic amplification occurs to that in which it doesn't then clearly the accelerations have to become more uniform.

Dynamic elasto-plastic numerical analyses were performed. These analyses illustrated that without mitigation, the topography amplifies considerably the acceleration at the location of the building under two input earthquake motions. Parametric analyses illustrated the optimum configuration for the mitigation measures considered. When the optimum mitigation configurations are applied, the intensity of the seismic motion below the building approaches the levels of the 1-dimensional case far away from the edge of the slope, by about 50% or more. More specifically, in the cross-section of the slope, 20 anchors 5m apart proved more effective than 6 piles of similar length and spacing. More dense spacing near the building was even more effective in mitigating the seismic motion below the building.

6. ACKNOWLEDGEMENTS

The work was funded by the European Commission, Direction General XII for Science, Research and Development (Project no G1RD-CT-2002-00702). Dr G. Madabhushi and Dr A. Brennan of University of Cambridge, U.K. and Mr Jean-Pierre Hamelain of Soletance-Bachy, France assisted in proposing and designing the mitigation measures. Mr Aris Stamatopoulos provided valuable comments. Prof. Pitilakis of Aristotle University of Thessaloniki assisted in the selection of accelerograms and provided the histories. IGME provided topographic and geotechnical data of the site under consideration.

7. REFERENCES

- Athanasopoulos, G.A., Pelekis, P.C., Leonidou, E.A., "Effects of surface topography on seismic ground response in the Egion (Greece) 15 June 1995 earthquake," *Soil Dynamics and Earthquake Engineering* 18, 135-149, 1999.
- Assimaki D., Kausel E., Gazetas G., "Wave propagation and soil-structure interaction on a cliff crest during the 1999 Athens Earthquake", *Soil Dynamics and Earthquake Engineering* 25, 513-527, 2005.
- Aubry, D., Benzenati, I. and Modaressi, A., "Numerical predictions for model No 1, Verification of numerical procedures for the analysis of liquefaction problems," Arulanandan K. and Scott R. F. (editors), Balkema, Rotterdam, 45-54, 1993.
- Bouckovalas, G.B., Gazetas, G. and Papadimitriou, A.G., "Geotechnical aspects of the 1995 Aegion, Greece, earthquake," 2nd International Conference on Earthquake Geotechnical Engineering, Seco e Pinto, Balkema, Rotterdam, 1999.
- Bouckovalas, G.D. and Papadimitriou, A.G., "Numerical evaluation of slope topography effects on seismic ground motion," *Soil Dynamics and Earthquake Engineering; Issues 7-10*, August-October, Pages 547-558, 2005.
- BRGM (French Geological Survey) Software, "Cyberquake, Version 1.1. User's Guide," France, 1998.
- ITASCA Consultants, "FLAC (Fast Lagrangian Analysis of Continua), S. A., Version 4.0," 2002.
- Ishbashi, I., and Zhang, X., "Unified dynamic shear moduli and damping ratios of sand and clay," *Soils and Foundations*, Vol. 33, No. 1, 182-191, 1993.
- Modaressi, A. and Lopez-Caballero, F., "Global methodology for soil behavior identification and its application to the study of site effects," *Proceedings: Fourth International Conference of Recent Advances in Geotechnical earthquake engineering (CD-ROM)*, March, San Diego, California, 2001.
- Stamatopoulos, C., Bassanou, M., Poyadji, E., Kynigalaki, M., "Elastoplastic dynamic analysis of the Aegion slope during the 1995 earthquake," *The 11th International Conference of IAMAG, the International Association of Computer Methods and Advances in Geomechanics*, June, Torino, Italy, 2005.
- Stamatopoulos, C., Bassanou, M., Madabhushi, G., Brennan, A., "Evaluation of an elastoplastic method for simulating the seismic response of dense slopes using centrifuge test data," *The 11th International Conference of IAMAC*, Torino, Italy, 2005.